

PROCEEDINGS OF SPIE

SPIDigitalLibrary.org/conference-proceedings-of-spie

GPI 2.0: design of the pyramid wave front sensor upgrade for GPI

Fitzsimmons, Joeleff, Agapito, Guido, Bonaglia, Marco, Boucher, Marc-André, Chilcote, Jeffrey, et al.

Joeleff Fitzsimmons, Guido Agapito, Marco Bonaglia, Marc-André Boucher, Jeffrey Chilcote, Jennifer Dunn, Simone Esposito, Guillaume Filion, Dan Kerley, Quinn Konopacky, Jean-Thomas Landry, Olivier Lardiere, Bruce Macintosh, Alex Madurowicz, Jerome Maire, Christian Marois, Lisa Poyneer, Dmitry Savransky, Jean-Pierre Veran, "GPI 2.0: design of the pyramid wave front sensor upgrade for GPI," Proc. SPIE 11448, Adaptive Optics Systems VII, 114486J (13 December 2020); doi: 10.1117/12.2563150

SPIE.

Event: SPIE Astronomical Telescopes + Instrumentation, 2020, Online Only

GPI 2.0: Design of the Pyramid Wave Front Sensor upgrade for GPI

Joeleff Fitzsimmons^{a*}, Guido Agapito^b, Marco Bonaglia^b, Marc-André Boucher^h, Jeffrey Chilcote^c, Jennifer Dunn^a, Simone Esposito^b, Guillaume Filion^h, Dan Kerley^a, Quinn Konopacky^d, Jean-Thomas Landry^h, Olivier Lardiere^a, Bruce Macintosh^e, Alex Madurowicz^e, Jerome Maire^d, Christian Marois^a, Lisa Poyneer^f, Dmitry Savransky^g, Jean-Pierre Veran^a

^aNational Research Council Canada – HAA, 5071 West Saanich Road, Victoria, B.C. Canada, V9E 2E7;

^bINAF – Arcetri, Largo Enrico Fermi 5, I - 50125 Florence, Italy

^cNotre-Dame University

^dUC – San Diego, Center for Astrophysics and Space Sciences

^eStanford University

^fLawrence Livermore National Laboratory

^gCornell University

^hOMP Inc., 146 Bigaouette St. Quebec City, QC, Canada, G1K 4L2

ABSTRACT

After more than six years of successful operation at Gemini South, the Gemini Planet Imager (GPI) will be moved to Gemini-North. During this move, the instrument will undergo a series of upgrades. One of these upgrades will be the installation of a new pyramid wavefront sensor (PWFS) with a low noise EMCCD detector that will replace the current Shack-Hartmann WFS. This upgrade is expected to significantly increase the sky coverage of GPI, providing increased level of AO correction and access to fainter targets. The new PWFS will be assembled on a standalone bench that will be aligned and tested independent of the GPI to ensure the required performance is achieved. Once the performance is verified, the completed subassembly will be installed in place of the current WFS hardware during the final integration into the GPI.

In this paper, we will present the final design of the new GPI PWFS. Included will be a description of the optical performance simulations completed and their results, and a detailed overview of the opto-mechanical design of the new PWFS bench.

Keywords: Gemini, GPi, Pyramid WFS, Optical, Mechanical, Design, Analysis

1. INTRODUCTION

The Gemini Planet Imager (GPI) is a facility-class instrument that was originally designed for and installed on the Gemini-South 8 meter telescope located in Chile. Since the commissioning of GPI in 2013 and the beginning of science operations in 2014, GPI has been used for a wide range of scientific programs ranging from large-scale exoplanet surveys to short-term, high-impact observations leading to the discover of new exoplanets.^[1] The GPI instrument consists of three major components: an adaptive optics (AO) system, a calibration (CAL) system and an integral field spectrograph (IFS). These systems work together to correct the bulk atmospheric distortions, attenuate the light from the star while transmitting the light from any nearby orbiting exoplanets, correct any residual aberrations not corrected by the AO system and complete the spectral analysis of the remaining exoplanet light.

With the decision to move GPI to Gemini-North, the scientific community decided to leverage this opportunity by embarking on a significant upgrade to several GPI systems that will further enhance the capabilities of the new GPI2. The portion of the GPI2 upgrade that is covered in this study is the AO system upgrade. The original AO system, based on a Shack-Hartman wavefront sensor (WFS) design, will be replaced with a new AO system utilizing a pyramid WFS (PWFS) which will enable access to lower magnitude stars while providing better correction than GPI is currently capable of delivering. Significant effort has already been expended to validate the PWFS concept through analysis and testing completed during the development of the PWFS design for the Thirty Meter Telescope's (TMT) Narrow Field InfraRed Adaptive Optics System (NFIRAOS). Leveraging this work, using many of the same components designed for

NFIRAOS, will provide a robust upgrade to GPI. The contents of this paper will describe the optical design and supporting simulations, and the final opto-mechanical design of the GPI2 PWFS AO system

2. OPTICAL DESIGN AND SIMULATION

2.1 PWFS Optical Design

The optical design concept, illustrated in Figure 1 below, receives an f/64 beam reflected from the GPI science beam-splitter (dichroic with a cut-off wavelength of 925nm) that passes through two flat steering mirrors: one with two angular adjustments (SM1) and one with two angular adjustments plus one linear adjustment to control focus (SM2). These two mirrors adjust the position and focus of the spot on the tip of the pyramid (pointing) as well as the position of the pupil images on the detector (centering). Additionally, SM1 is used to modulate and dither the spot around the tip of the pyramid. The pyramid optic is a glass double-pyramid that splits light into four channels, each of them going through a lens (camera lens) to create an image of the telescope entrance pupil onto a fast-readout low-noise detector (EMCCD) for image acquisition. Close to the tip of the pyramid, a field stop limits the FOV to reduce background contamination and limit source confusion. Absent from this design is an atmospheric dispersion compensator unit (ADC) since the expectation is to use the GPI wide-band ADC in the common path. The feasibility of using the GPI ADC was a significant risk in this design and was addressed first in the development of the GPI2 PWFS upgrade. This work is summarized in Section 2.3 below.

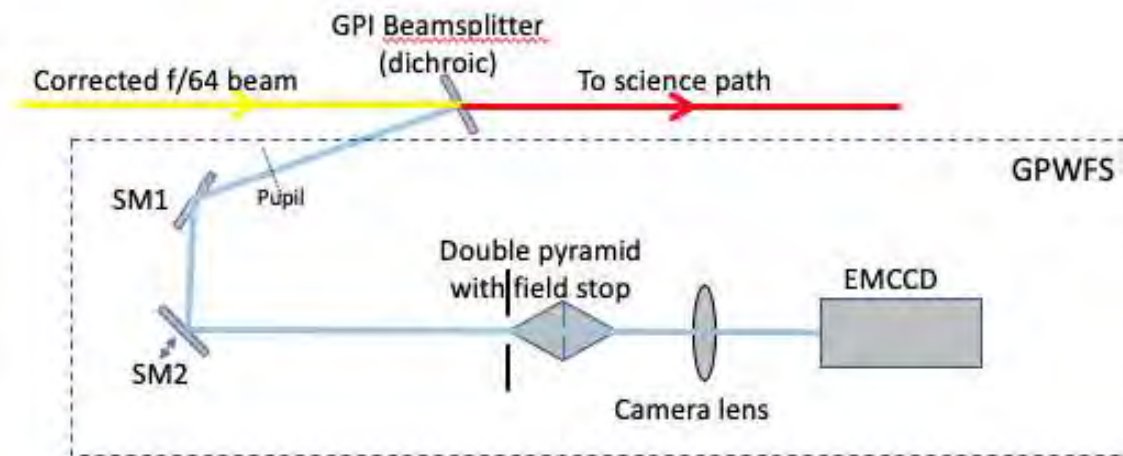


Figure 1. GPI2 Pyramid WFS optical layout.

The tip and tilt actuation for the two steering mirrors (SM1 and SM2) are provided by two identical fast steering mirror (FSM) actuators (PI S-331.5SL) that can operate up to 2000 Hz. The selected PWFS detector is a frame-transfer EMCCD which operates at frame rates between 10Hz and 2000 Hz, depending on the magnitude of the NGS. The images recorded on the PWFS detector are sent to the Real Time Computer (RTC), where they are processed to control the GPI woofer deformable mirror (DM), the GPI tweeter DM and the Tip-Tilt Platform.

As illustrated in Figure 1, FSM1 is located near a pupil plane and can move the image at the tip of the pyramid. In this manner, FSM1 is used to introduce a fast modulation of the position of the spot (image of the NGS) with respect to the tip of the pyramid. This modulation consists of applying two sinusoids in quadrature to the two axis of FSM1, so that the spot position follows a circle around the tip of the pyramid. The typical radius of this modulation circle is three times the width of the spot ($3 \cdot \lambda/D$). The modulation must be tightly controlled so that the spot describes an integer number of circles (usually one) during the integration time on the detector, which is equal to the inverse of the frame rate, and therefore can be as small as 500 μ s (goal 333 μ s). Each circle must have very low distortion to precisely distribute the light among the four pupil images. This precise distribution is a fundamental precondition for the measurement algorithm; thus the commands to FSM1 are highly oversampled compared to the frame rate.

On top of the fast modulation, a slower modulation (dither) can be added. This slower modulation, which is called dithering, also consists of applying two sinusoids in quadrature to the two axes of FSM1, except that the period of the sinusoids is at least four times the detector integration time, i.e. ≥ 2 ms. Again to prevent distortion, the time between two consecutive FSM1 dither command updates may need to be shorter than one CCD integration time.

The implementation of the optical design within the constraints of the space envelope available for the PWFS upgrade required that the final design contains two additional fixed fold mirrors. As illustrated in Figure 2, a linear stage for focus adjustment will be implemented on the first fixed fold mirror. Further details regarding the implementation of these components is provided in the Opto-Mechanical Design section below.

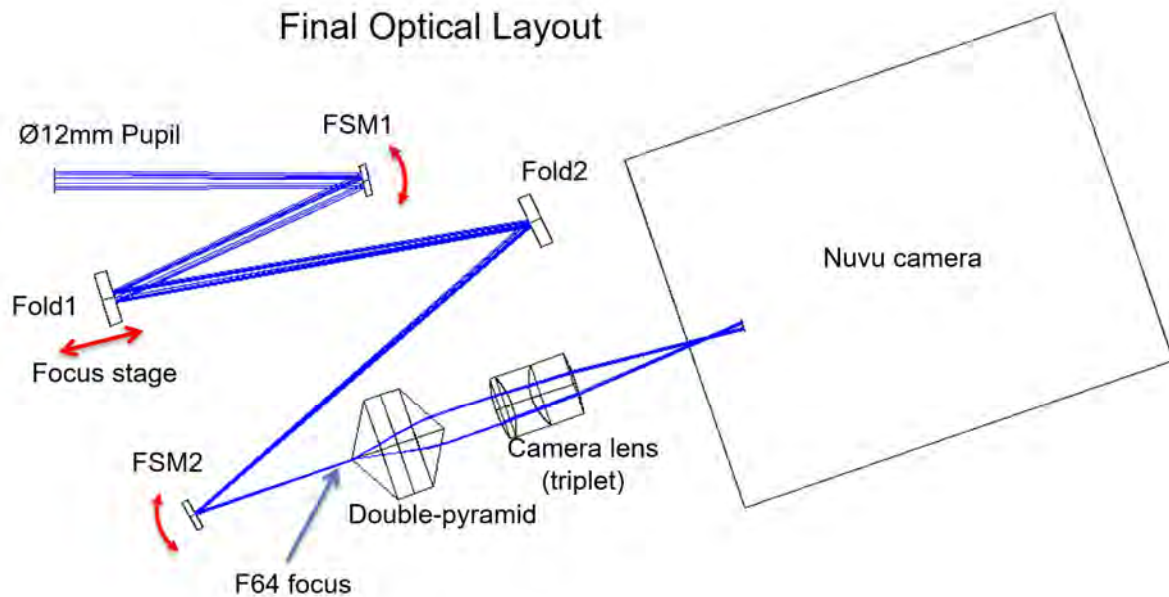


Figure 2. Schematic layout of the final optical design for the PWFS upgrade.

2.2 PASSATA

The AO simulation software used to support the GPI2 PWFS design is PASSATA, developed in IDL by the Arcetri Observatory Group. PASSATA has been specifically designed to simulate a PWFS and has been used extensively to simulate the LBT AO systems. It has been configured to simulate GPI 2.0 with the PWFS, and has been modified to include implementation defects specifically tailored for GPI, including blur from incomplete ADC corrections, pyramid defects, pupil image centering errors, pupil plane distortions, and dead DM actuators.

2.3 Atmospheric Disturbance Compensator Feasibility Study

A key element of the GPI PWFS modeling study was to verify that the existing GPI ADC, located in the common path, would be suitable for operation with the PWFS. This ADC was designed to be broadband, but with a Shack-Hartmann WFS, the spot quality required at the WFS wavelength is much less than for the PWFS. Also, we wanted to make sure that the as-built ADC (measured during the integration and testing of GPI at NRC-HAA) would be suitable for operation in the science bands, with the atmospheric conditions specific to Mauna Kea. The bulk of this work was completed by the INAF-Arcetri group and involves an optical study to determine the optimal control law for the separation of the two ADC prisms, as well as the use of PASSATA to determine the effect of the residual dispersion error on the AO performance.

The GPI ADC is a linear ADC made of two double prisms. Each double prism assembly can be independently rotated. These double prisms need to be jointly rotated when the Cass rotator angle changes. However, since the Cass rotator angle is fixed during all GPI observations, the prism assemblies are never rotated. The relative rotation between the two

prisms has been set to 3.5° in order to minimize the as-built errors. This rotation is included in the as-built Zemax prescription file used for these analyses.

The separation between the two prism assemblies provides power to compensate for dispersion and is adjusted as the zenith angle changes. The exact control law (separation versus zenith angle) can however be optimized to minimize the dispersion in a given science band (Y-J-H-K or broadband, i.e. across all the science bands). The optimized control laws are presented in Figure 3.

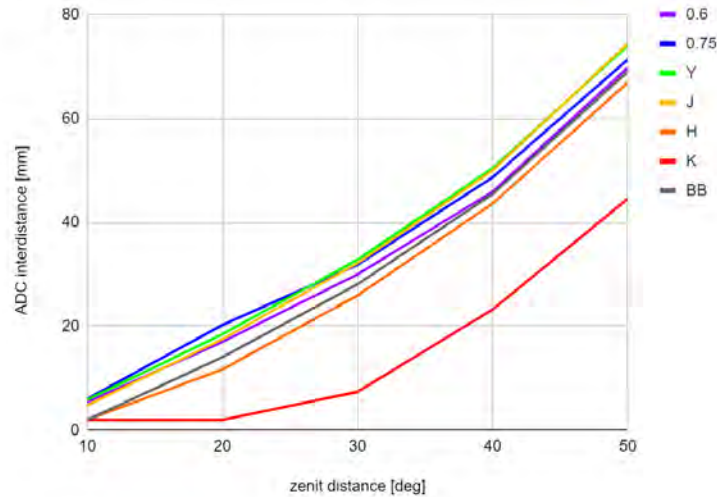


Figure 3. Optimized control laws for ADC element separation as a function of zenith angle.

Although there were no formal requirements and metric defined for the in-operation performance of the ADC, Bruce Macintosh provided the following guidance:

“For the science path we should have a dispersion of no more than $0.1 \cdot \lambda/D$ when optimized for one band and no more than $0.2 \cdot \lambda/D$ for broadband observations, although these requirements could probably be relaxed by x2 if needed.”

Throughout the ADC simulation process, the following metrics are used to quantify the residual distortion:

- The maximum distance between chief rays (P-V)
- $2 \cdot S = 2 \cdot \text{RMS}$ distance between chief rays (this metric seems to be the most relevant)

The residual dispersion from the optimized control laws for ADC optimization at each band were calculated (see Table 1). When using the $2 \cdot S$ metric, the requirement is met at J, H and K bands, whereas the x2 relaxation is needed to meet the requirement at Y band and in broadband mode. We conclude that the ADC works well for the science bands, including broadband.

Table 1. Residual dispersion estimated for the optimization of the ADC for various bands.

ADC optimization band	C. wave [um]	L/D [mas]	Dispersion PTV		Dispersion 2*S	
			[mas]	[L/D]	[mas]	[L/D]
Y	1.020	26.28	4.93	0.19	3.37	0.13
J	1.220	31.43	3.43	0.11	2.36	0.07
H	1.630	42.00	1.92	0.04	1.40	0.03
K	2.190	56.42	8.12	0.14	5.57	0.10
Broadband	1.730	44.57	19.00	0.43	13.24	0.30

Additional studies were completed to assess the residual dispersion when the ADC is optimized for the PWFS band and it was concluded that the best performance is achieved by using the broadband optimizations which results in a maximum residual dispersion of 50 mas P-V at the tip of the pyramid. This residual dispersion corresponds to $2/3$ of the nominal modulation radius ($3\lambda/D$) which slightly reduces the PWFS sensitivity and thus slightly increases noise propagation on bright NGSs. However, subsequent simulations using PASSATA show that the impact on AO correction performance is negligible.

The final conclusion from the ADC feasibility study is that the GPI ADC will perform sufficiently well allowing the PWFS upgrade to achieve its intended performance requirements.

2.4 PWFS Optical Design and Tolerances

Pupil Image Positions

During the conceptual design phase for the GPI PWFS, the requirement on the exact position tolerances for the four pupil images on the detector was relaxed to allow the angular tolerances of the pyramid faces to be set to a few arcmin so that the cost of these component can be significantly reduced. In a traditional PWFS (Fried geometry), the pupil images must be separated by an integer number of pixels leading to very tight tolerances on pyramid face angles (\sim a few arcsec) making the manufacturing very difficult and expensive. During the NFIRAOS PWFS design study, analyses have shown that relaxing these tolerances has negligible consequences as long as the number of pixels in the diameter of each pupil image significantly exceeds the number of actuators (i.e. the PWFS is significantly over-sampled compared to the minimal Fried geometry). This was again verified using PASSATA for the GPI2 PWFS, which has 60 pixels for 44 actuators across the diameter.

Pupil Image Blurring

Several factors contribute to blurring the pupil images, including lateral color, residual pupil motion during modulation, and charge diffusion between pixels. The GPI2 PWFS design requirements set a top-level number for the permissible blurring and discussed how this number is broken down into different items. PASSATA has been used to verify that this top-level number produces negligible performance degradation. While the blurring reduces the sensitivity of the PWFS to high-order modes and increases the noise propagation accordingly (see Figure 4), the final impact on the WFE is very small (see Figure 5).

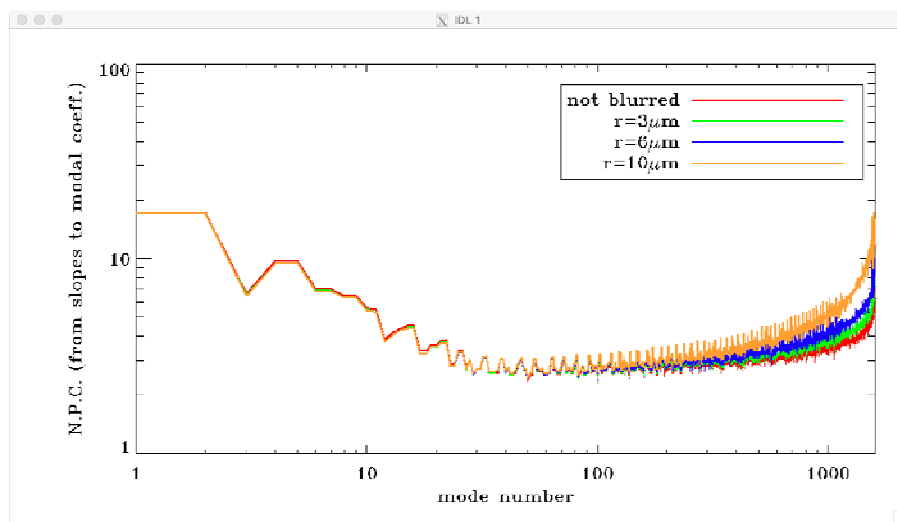


Figure 4. Effect of pupil blurring on noise propagation.

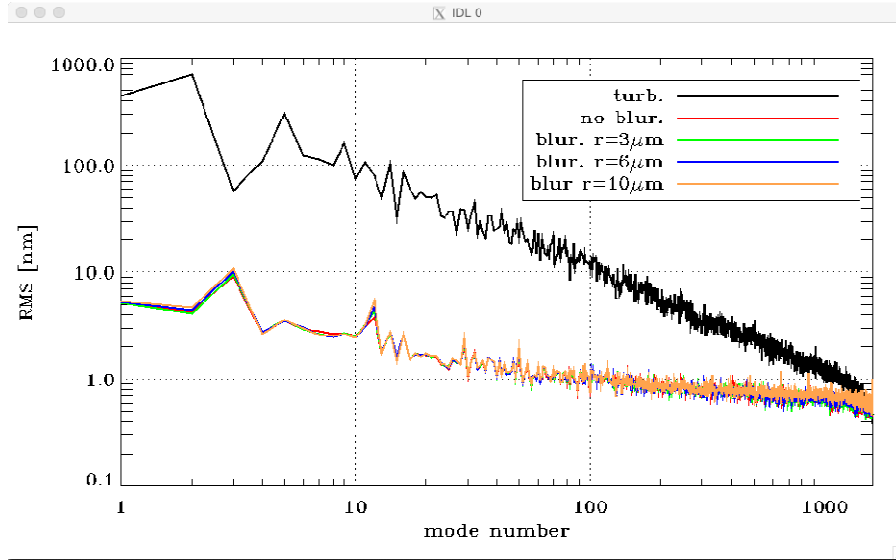


Figure 5. WFE impact of pupil blurring

2.5 End-to-End Simulations

After assembling and validating all the simulation components, PASSATA was finally used to complete several end-to-end simulations of the GPI2 PWFS performance once installed in the as-built GPI instrument.

Performance versus Guide Star Magnitude

The GPI2 AO performance has been evaluated for different guide stars and for various conditions so that the performance sensitivities to various parameters could be determined. Figure 6 (a) & (b) illustrate some of the performance sensitivities that were completed, showing the performance for control loop frequency and atmospheric seeing, respectively. The point spread functions, shown in Figure 7, illustrate the performance impact of the gain settings. Upon completion of an extensive suite of simulations, the results clearly demonstrate that GPI2 will be able to operate on stars between $I=0$ and $I=14$ and that the performance will degrade gracefully for magnitude larger than $I=13$. Note that the simulation assumes a 300nm bandpass for the PWFS (600nm-900nm) and a global throughput attenuation factor of 0.32 [from the estimated throughput of 0.83 (Telescope), 0.72 (AO relay), 0.8 (PWFS path) and 0.73 (EMCCD)].

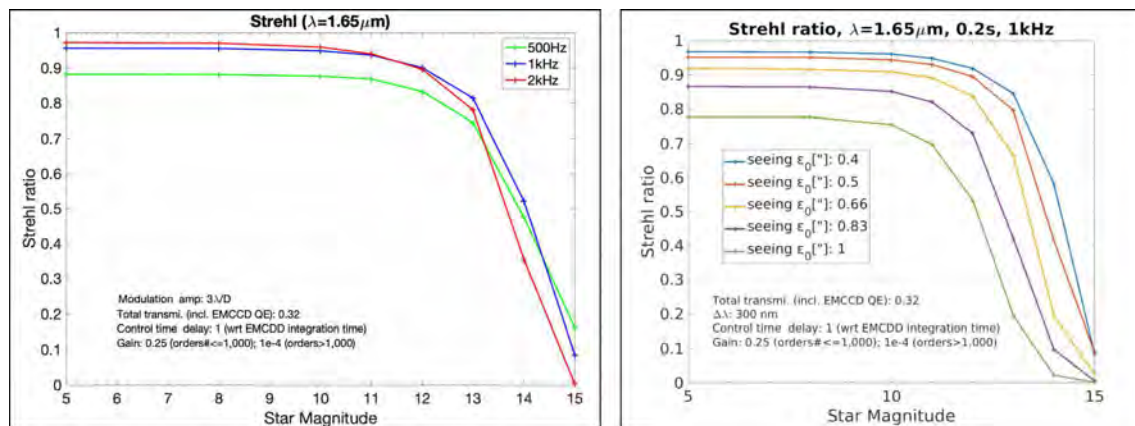


Figure 6. (a) The left-hand plot illustrates the Strehl ratio as a function of control loop frequency; (b) the right-hand plot illustrates the impact of atmospheric seeing on the Strehl ratio.

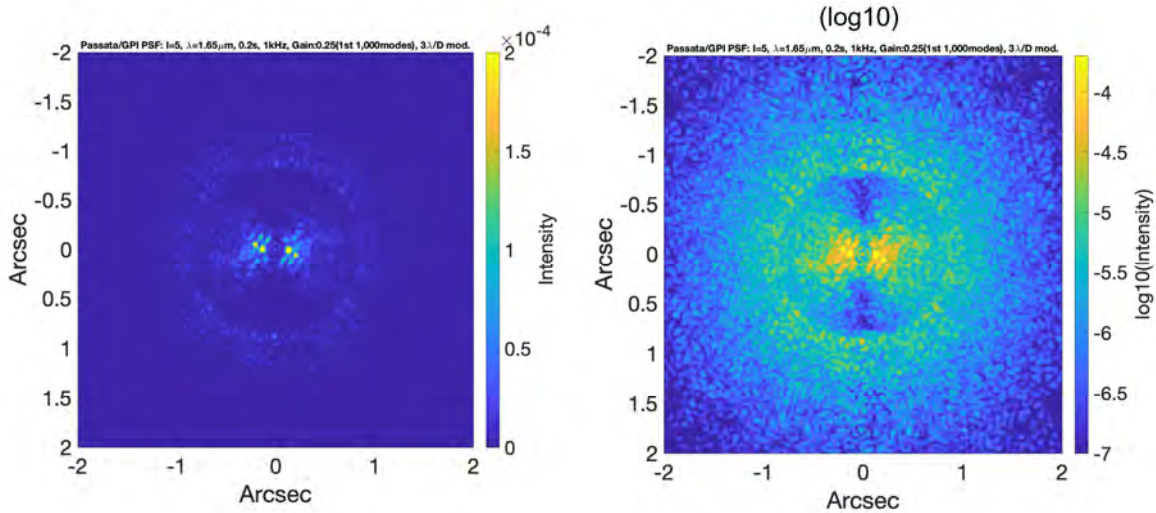


Figure 7. The occulted Point Spread Functions (PSF) for integrator gains set to 0.25 (mode # < 1000) and -0 (mode # > 1000), shown left and right, respectively.

Effect of M2 Print-Through

The effect of M2 print-through is expected to have a non-trivial impact on the performance of GPI2 installed on Gemini-North. The potential significance of this performance impact was assessed using PASSATA. The wavefront map used to model the print-through come from an on-sky measurement by Olivier Lai using curvature sensing (see Figure 8). The results of these simulations show that the M2 print-through effect severely degrades the delivered contrast (see Figure 9) by up to a factor two.

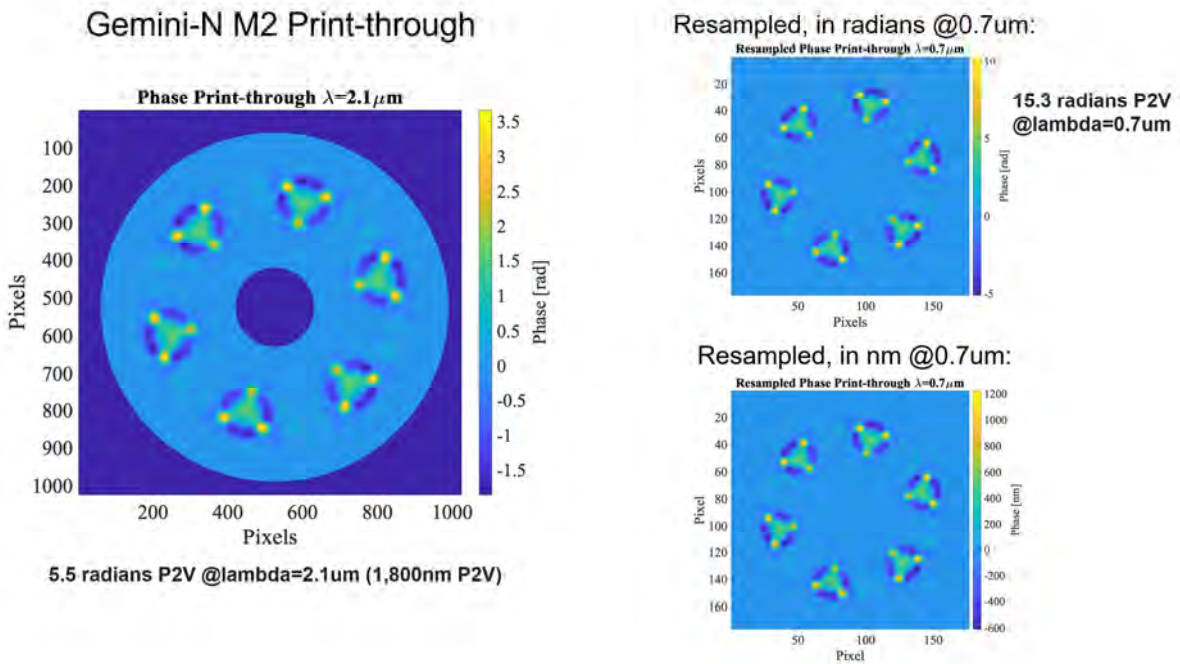


Figure 8. Wavefront map of the measured print-through on the Gemini-North secondary mirror (M2)

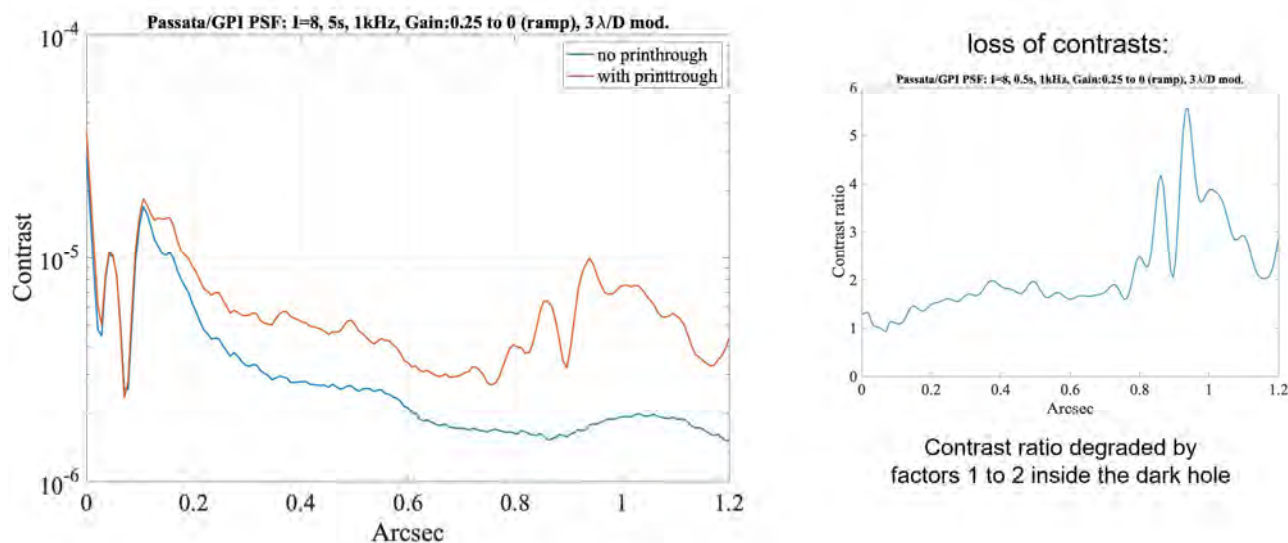


Figure 9. Contrast ratio degradation due to Gemini-North M2 print-through

3. PWFS OPTO-MECHANICAL DESIGN

3.1 Upgrade Considerations

As the optical design entered the final stages, the opto-mechanical packaging design began. One of the major risks with upgrading any existing instrument is the possible discrepancy between the expected design and the as-built instrument. In this case, this risk is greatly mitigated due to the extensive testing and measurement of the as-built GPI AO system completed at NRC-HAA prior to integration of the instrument at Gemini-South. These measurements include the precise locations of the delivered optical path (beam, focus and pupil locations) of the entire AO system with respect to known datums located on the AO bench. The location of the new PWFS components must be installed within the region where the SHWFS components currently are mounted characterized by the space envelope detailed in Figure 10. Also, in order to facilitate the upgrade and enable concurrent fabrication, assembly, alignment and testing of all aspects of the GPI2 upgrade, the PWFS system must be self-contained allowing the off-line alignment and testing prior to installation on the GPI AO bench. This requirement dictated that the PWFS system be assembled on a separate PWFS bench that will be mounted and aligned to GPI as a single subassembly.

Concurrent with the design phase of the PWFS, the WFS camera was also under development at NuVu. A major complicating factor in the opto-mechanical design was the progressive enlargement of the NuVu camera envelope compared to the original estimated size. Once the external dimensions and primary interface features of the NuVu camera were confirmed, many different optical layouts and fold mirror configuration scenarios were traded until a design was achieved that met the all the requirements. The final design includes two additional manually-adjustable fold mirrors which provides a beneficial alignment correction potential since it can correct any kind of beam misalignment by design (see final layout illustrated in Figure 2).

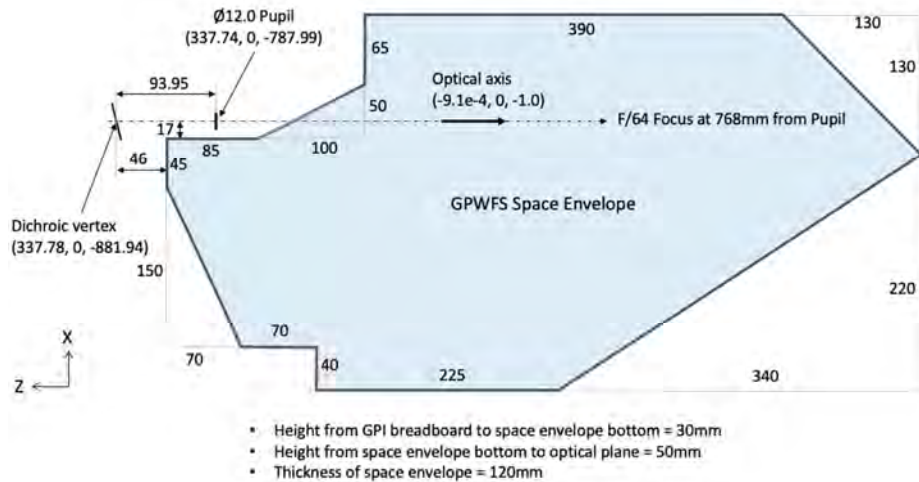


Figure 10. Space envelope available for the installation and configuration of the PWFS opto-mechanical components.

Despite the extensive design iterations, there still remains limited room behind the camera, which must be considered by NuVu when selecting the connectors and service bending radii for the final camera design. At the time of writing there remains several outstanding camera details that will be required to proceed with full fabrication of all components.

3.2 Mechanical Design

The PWFS opto-mechanical design, illustrated in Figure 11, consists of a monolithic aluminum bench, two FSMs, two manually-adjustable fold mirrors, the pyramid mount assembly, the camera lens mount assembly and the NuVu camera. When mounted in its nominal position on the GPI AO bench, the PWFS assembly maintains a 3mm margin with the space envelope providing a minimum of 8 mm of clearance to all other AO components (there is a 5mm clearance between the defined space envelope and the nearest component on the GPI AO bench). The PWFS assembly is mounted to the AO bench through the three system-level jacking sleeves that provide a rigid and stress-free connection when locked while providing 3 degrees-of-freedom (DOF) of adjustment with respect to GPI when unlocked. The other 3DOF are provided by the system-level nudgers affecting the position/rotation of the PWFS assembly on the GPI AO bench.

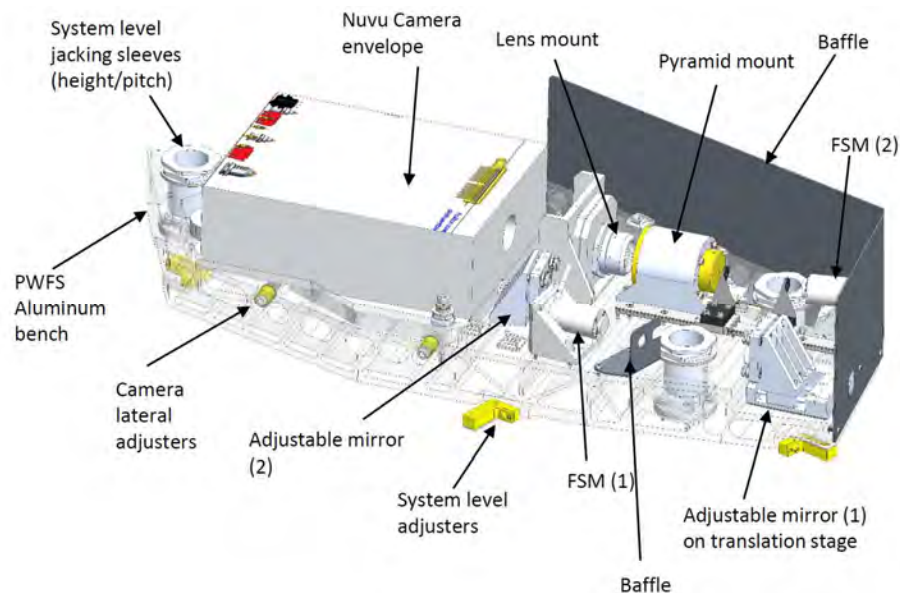


Figure 11. PWFS Subassembly view of the opto-mechanical design

The PWFS optical bench is a monolithic part machined from 6061-T6 aluminum. This material was selected for its excellent mechanical dimensional stability and for its coefficient of thermal expansion (CTE) that matches that of the GPI AO bench to which it will be mounted. The PWFS bench was designed as thick as possible within the current space envelope constraints to maximize the system natural frequencies. Additionally, the novel “sandwich-like” light-weighting pattern (Figure 12), offering better stiffness-to-weight ratio compared to an open-back structure, contributes to improved dynamic performance characteristics. Using triangular shaped cavities running the full width of the bench were found to provide the best stiffness-to-weight ratio.

This configuration also facilitates the use of short, stiff mounts between the PWFS bench and the GPI AO bench since the optical axis is near the bench surface. This also greatly increases the natural frequencies of the optical mount assemblies compared to the reference design which required more slender optical mounts. The bench provides a rigid base for mounting and aligning the PWFS optical assemblies separate from the GPI instrument facilitating the rapid integration of multiple upgrades simultaneously.

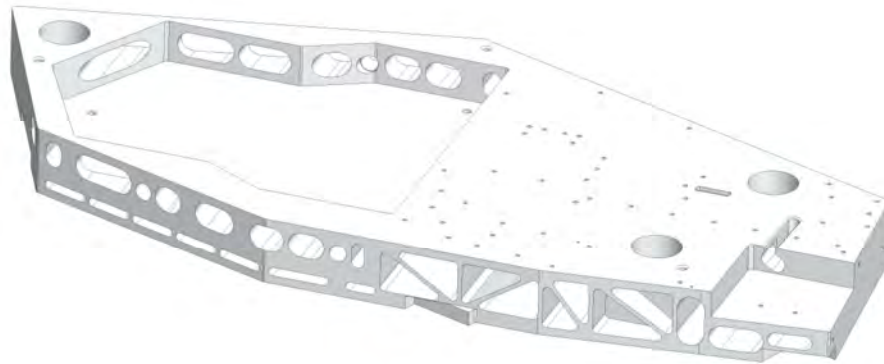


Figure 12. PWFS monolithic optical bench made from 6061-T6 Aluminum.

As illustrated in the optical layout (Figure 2), the first and last mirrors in the optical design are FSMs that use PI S331.5SL actuators each with a bonded mirror. Each PI actuator is mounted to a monolithic, thick-walled, aluminum mount pinned and bolted to the PWFS bench (Figure 13). The mirrors will be fused silica due to their COTS availability. Special care must be given to the process used to bond these mirrors to the PI actuators due to the high frequency operation. Two adhesives were considered for this interface: 3M Scotch-Weld 2216 B/A Gray epoxy adhesive and Dow Corning RTV 732. Based on a series of thermo-elastic and modal analyses to assess these two adhesives, the option to use the 3M 2216 epoxy adhesive was selected, in a configuration of six $\phi 2\text{mm}$ adhesive pads, due to the low thermally-induced surface error (4nm RMS) and stress (6 MPa). The modal analysis of this configuration confirmed the first natural frequency of the mirror is 19 kHz which is an order of magnitude larger than the operating frequency of 2 kHz.



Figure 13. FSM mount design

The second and third mirrors are adjustable folding mirrors using robust custom mounts (illustrated in Figure 14), inspired by commercial adjustable mirror mounts. This mount design will prevent misalignment during shipment and provide natural frequencies well above 2 kHz thus eliminating any chance of dynamic interaction with the FSM actuators. A COTS $\phi 1.0$ inch mirror is elastomerically mounted in the mirror plate using RTV adhesive introduced through radial injection holes. This mounting approach is the most robust and provides a low-stress mounting solution with negligible thermally-induced surface distortion. A single-component, low outgassing soft silicone, such as Dow Corning 732 or the more expensive Dow Corning 6-1104 can be used to bond these optics in place.

The mirror plate is attached to the mirror brace through three threaded sleeves each combined with spherical and wave washers to allow for tip and tilt adjustments without inducing mirror distortion. The mirror is adjusted by rotating the threaded sleeves and then locked in place using a lock nut. This process is more iterative than a simple COTS mount but also more robust. The wave washer in each sleeve eliminates the axial backlash in the threads of the sleeve, which eases the adjustment process. Belleville washers play the same role below the M3 fasteners heads. Once the desired alignment has been reached, lock nuts and fasteners are tightened to their prescribed torque resulting in a hard mount, free of balls or springs. The threaded sleeves have a $3/8''-100$ thread to provide the same resolution as standard COTS mounts.

One of the two mirrors is mounted on a PI M111.1-DG linear translation stage to provide focusing, axial scanning, and general adjustment of the optical path length.

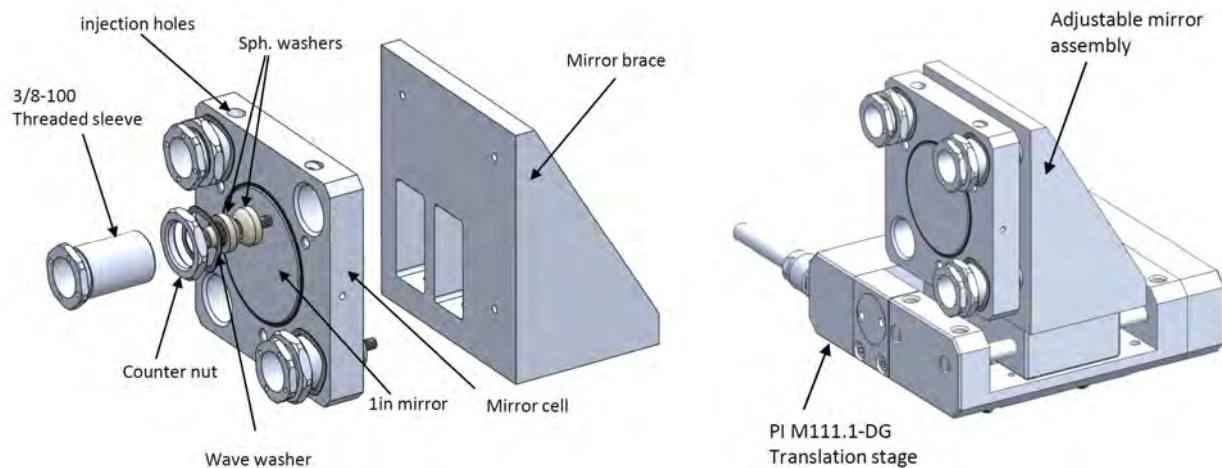


Figure 14. Manually-adjustable fold mirror mount design: exploded view and shown mounted on the linear stage.

Following the FSM2, the next optic in the PWFS system is the pyramid optic which is bonded assembly of two pyramid optics supported in a custom mount (illustrated in Figure 15). The pyramid is first held in place by using Torlon spherical seats that contact the pyramidal surfaces outside the clear aperture, hence providing a compliant polymer interface without over constraining the pyramid thanks to the integral spherical seats. Torlon engineering polymer has a CTE very close to aluminum which was the rationale for material selection. A slight axial preload of the pyramid optic is generated by a series of lightly preloaded wave washer (approximates a 2g load). This minimal preload facilitates the system testing, alignment and commissioning prior to final bonding. The slight preload allows various operating orientations while still inducing negligible strains in the pyramid. The pyramid can be clocked using a spanner wrench to adjust indexation relative to its housing.

The pyramid is bonded inside its aluminum housing using ‘radially-oriented RTV silicone dots on the square portion of the pyramid as shown in Figure 15. This portion of the pyramid is not part of the optical system and has no edge blackening paint. The same RTV specified for the FSMs and fold mirrors, can be used in the bonding of the pyramid optic. The design includes “inspection windows” to monitor the diameter of the RTV dots while injecting (the injection is stopped when dots are tangent to the windows).

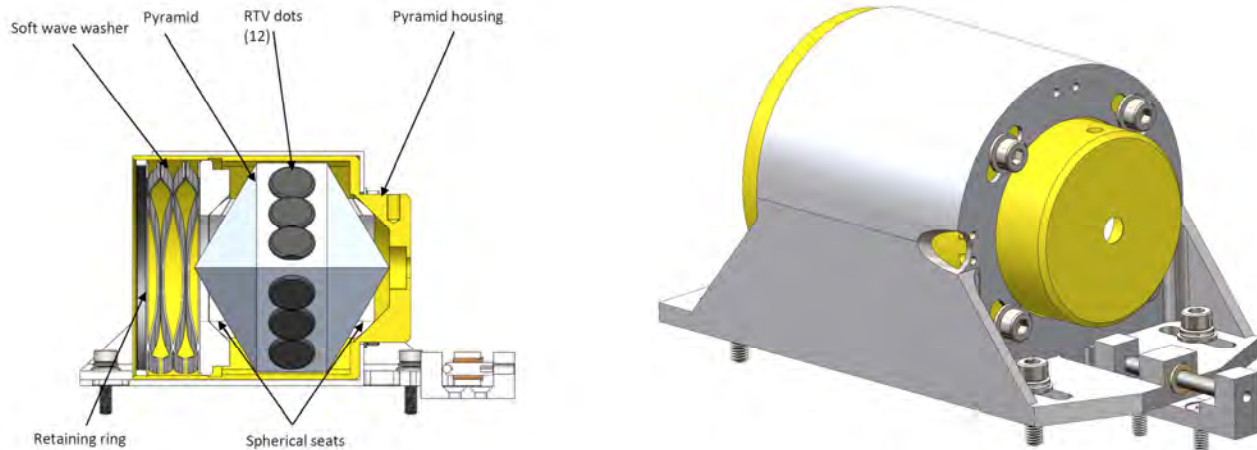


Figure 15. Pyramid optic mount design.

Once the pyramid is bonded in its housing, the resulting assembly is mounted flat directly on the bench, aligned by dowel pins in slots, and its axial (Z) position is adjustable using a 0.2mm pitch COTS adjustment screw. To ease adjustment, Belleville washers lightly preload the housing on the bench. After the adjustment is completed, the fasteners are tightened resulting in a very stiff mount interface without any balls or springs, just a solid aluminum contact. This design delivers an adjustable mount with the stiffness of a hard mount.

The last optical mount in the PWFS system, the camera lens mount, builds on the same design philosophy already incorporated into the other optical mounts. The camera lens mount provides adjustment in three orthogonal axes by using three stacked linear adjustment screws (see Figure 16). The lens is elastomerically mounted using RTV dots as described previously. Similar to the pyramid optic mounting scheme, a “hard” mechanical mount for testing and commissioning is created by implementing a spherical interface at one end of the lens (corresponding to triplet optical surface), a polymer retaining ring and a controlled mechanical gap around the lens. In this way, the lens can be inserted and gently mounted as with standard lab mounted optics and then RTV dots can be injected when ready. The three orthogonal degrees of freedom (X, Y and Z translation) adjustment is performed using the three linear adjuster. Extra adjustment range along the optical axis is available by threading the lens cell and locking it where desired using lock nut. Fine tuning is done using XYZ translation mechanism.

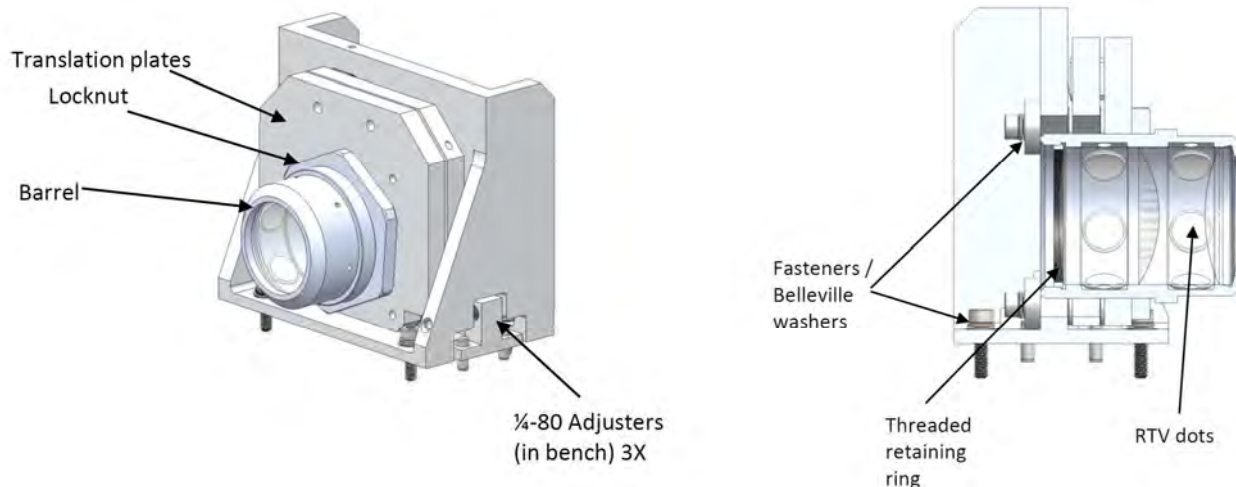


Figure 16. Camera Lens adjustable mount design

Finally, the stray-light baffling requirements for the PWFS upgrade needed to be addressed. Although these were not well defined, the design approach used was to provide as good or better baffling compared to that provided in the SHWFS implementation. The layout shown in Figure 17, provides a significant increase in stray-light baffling with respect to the rest of the GPI science optical path while staying within the allowable space envelope for the PWFS system.

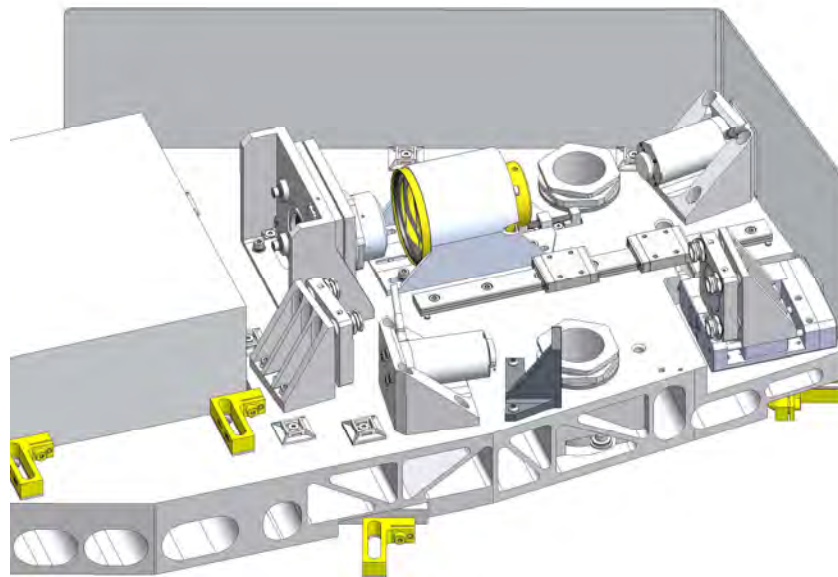


Figure 17. Stray-light baffling arrangement

CONCLUSION

Included as part of a major upgrade to GPI, the new PWFS AO upgrade will provide significantly improved performance for GPI2 when it is installed at Gemini-North. The extensive simulation work completed using PASSATA and the collaborative approach to the optical and opto-mechanical designs resulted in a compact, robust design upgrade that can be assembled, integrated and tested in parallel to other planned upgrades to GPI and then can be integrated together just prior to shipping GPI2. Extensive effort was allocated to developing and validating the alignment plans to ensure that the design not only met the performance requirements for the GPI2 upgrade but also could be easily assembled, aligned and tested independent of other GPI systems.

REFERENCES

- [1] Chilcote, Jeffrey K., Bailey, V. P., De Rosa, R., Macintosh, B., Nielsen, E., Norton, A., Millar-Blanchaer, M. A., Graham, J., Marois, C., Pueyo, L., Rameau, J., Savransky, D., Veran, J. P., "Upgrading the Gemini planet imager: GPI 2.0," Proc. SPIE 10702, Ground-based and Airborne Instrumentation for Astronomy VII, 1070244 (6 July 2018); <https://doi.org/10.1117/12.2313771>
- [2] Fillion, G., Boucher, M. A., Landry, J. T., "GPI2 Pyramidal Wavefront Sensor Design Report", OMP Inc., Quebec City, Quebec, Canada, A0585 FDR Report for NRC-HAA, 2020.
- [3] Veran, J. P., Maire, J., Agapito, G., "GPI2.0 Modeling and Requirements Definition Report", FDR Report for NRC-HAA, 2020.